Novel Nanocomposite Biomaterials to Control Cell Adhesion

Constança Júnior

Instituto Superior Técnico, Lisboa, Portugal

June 2017

Abstract

The diverse properties that hydrogels possess have been arousing great interest for many years due to their several biomedical applications, such as drug and cell carriers or as tissue engineering matrices. They possess the capacity of retaining up to a thousand times their dry weight in water, which added to their three-dimensional porous structure, confers them the ability to mimic native tissue microenvironment. Some of these properties are easily tunable, which makes it possible for researchers to manipulate certain characteristics. Poly(ethylene glycol) (PEG) is an intrinsically non-immunogenic, non-adhesive hydrogel, that has been widely used as a biomaterial. By undergoing chemical and physical modifications, it is possible to confer PEG-based hydrogels new properties that allow to widen their spectrum of applications in tissue engineering and regenerative medicine. One of those modifications can be the addition of different types of nanoparticles. In this work, approaches to combine spherical gold nanoparticles and gold magnetic nanoparticles with PEG-based hydrogels are reported. These nanocomposites aim to control the adhesion, proliferation and viability of mouse fibroblasts by allowing cells to interact with the gold of the nanoparticles. The topographical and mechanical characterization of the materials showed that the presence of nanoparticles in the volume of the hydrogel does not improve its stiffness, but influences the roughness of its surface and swelling behaviour. Cells showed little adhesion to the nancomposites, due to the lack of ability to expose the nanoparticles to the surface of the films.

Keywords: hydrogel, PEG, nanocomposite, gold nanoparticles, cell adhesion

1. Introduction

Generically, a biomaterial can be defined as a *" material intended to interface with biological systems to evaluate, treat, augment or replace any tissue, organ or function of the body"* [1]. Biomaterials possess the ability to be integrated in a biological system without interacting negatively with it, and therefore require to have certain mechanical, chemical and biological properties depending on their final application [2]. In 1960 a publication by Wichterle and Lim reported the synthesis of hydrogels for biological use [3], which triggered an increase on interest in exploring the use of hydrogels as a biomaterial, due to their hydrophilic character, chemical stability and ability to be biocompatible [4]. From the variety of hydrogels available, the use of poly(ethylene glycol) (PEG) as a biomaterial is especially interesting due to its ease to be manipulated. However, PEG itself is non-adhesive, which makes it necessary to adopt strategies that allow to provide them features that enable their successful application to control cell adhesion, migration, growth and to investigate fundamental cellular behaviour. Some of these strategies are based on the creation of topographical, chemical and elastic profiles [5, 6]. The incorporation of gold nanoparticles (AuNPs) in PEG-based hydrogels, resulting in new nanocomposite (NC) hydrogels, has shown to be a promising way of creating materials that induce physiological responses in biological tissues [7].

Having taken into account the advantages these materials present, this work follows the trend to develop PEG based biomaterials micropatterned with AuNPs and AuNMPs in order to control cell adhesion. Moreover, this work proposes a possible solution to integrate these nanoparticles in the matrix of the hydrogels conferring them new characteristics.

2. Theoretical Background

2.1. Hydrogels

Hydrogels are a group of polymeric materials, that due to their great hydrophilicity, have the ability to hold large amounts of water within their three-dimensional structures. They have the capacity of being highly biocompatible, which added to their easily tunable characteristics, allows the design and development of materials with tailored properties, such as biodegradation, mechanical stability, and ability to respond to stimuli [8]. Hydrogels can be synthetic, natural, or result from synthetic/natural polymer hybridization [9]. There are three general

components that take part on hydrogel preparation: monomer, initiator and cross-linker; and various polymerization techniques can be used, such as bulk, by irradiation, solution and suspension polymerization [8]. When talking about cell culture and the application of hydrogels as matrices or scaffolds, it is important to address its water absorption capacity as its ability to permeate the nutrients into and cellular products out of the gel. The amount of water imbibed within a hydrogel influences the diffusive properties of a solute through it. Thus, determining the amount of water imbibed is important to characterize the hydrogel, and is often represented in terms of percentage swelling ($\%S$). The $\%S$ can be defined by the following equation:

$$\%S = \frac{\mathrm{W_S} - W_d}{\mathrm{W_d}} \times 100 \quad (1)$$

where W_S is the weight of the swollen gel and W_d is the weight of the dry gel, which can be determined experimentally. The $\%S$ of a hydrogel is directly proportional to to the amount of water imbibed within it. The mechanical properties of the hydrogel depend on several factors, such as the monomers used, the polymerization conditions, the crosslinking density, the degree of swelling, and the type of medium in which the material is swollen. The size of the polymer molecules of the hydrogel leads to a viscoelastic response. Hydrogels are not simply elastic materials, but behave viscoelastically [10].

2.2. Gold Nanoparticles

When talking about biological applications of AuNPs, their shape, size and surface chemistry play an important role in determining their physiological behaviours and the way they will interact with proteins and cells. When proteins and other biomolecules are put in contact with AuNPs, they tend to be adsorbed to the surface of the nanoparticles and form a protein "corona" around them, which results in a reduction of their surface free energy. The size of the particles influences the amount of adsorbed protein on the surface due to the fact that different curvatures of the nanoparticles result in different protein binding constants. Smaller AuNPs have lower protein adsorption because of their larger curvature, which reduces the protein binding capacity. Thus, different factors may induce different cellular responses which can be used to mediate cell adhesion, migration, differentiation and proliferation [11].

2.3. Nanocomposite Hydrogels

Hydrogels, despite having easily tunable properties which make them suitable for various biomedical applications, have some constraints concerning their mechanical and physical properties to be used as tissue engineering scaffolds [12]. Several hydrogel preparation processes that aim to increase the stiffness of its networks have been developed, such as double network hydrogels, supramolecular hydrogels, microsphere cross-linked hydrogels and hybrid physically-chemically crosslinked hydrogels, presenting still, however, numerous limitations [13]. Thus, the incorporation of nanoparticles in the hydrogel matrix has arisen as a possible solution to overcome the mechanical limitations previously encountered. Also, it provides added potential use in biomedical applications for presenting superior chemical, physical, and biological properties, owing it to the characteristics that are inherent to the added material and the interactions between the polymeric networks and the nanoparticles [14].

The materials composing the NC hydrogel can vary immensely, and the different possible combinations of matrix and nanoparticles influence the characteristics that are later observed. Among the different types of particles, these can vary from carbon-based nanomaterials [15, 16], polymeric nanoparticles [17], inorganic nanoparticles [18], metal and metal-oxide nanoparticles [7].

2.4. Cell Adhesion Mechanisms

In order to maintain tissue strusture and mechanical integrity, it is essential for cells to adhere to their surroundings and to the extracellular matrix (ECM). The ECM is a complex network of proteins and polysaccharides secreted and assembled by cells which provides them with structural and biochemical support. Transmembrane cellcell and cell-matrix adhesion molecules provide a direct connection between neighbouring cells or ECM proteins and the cytoskeleton. These molecular networks assure structure, shape and mechanical strength. Moreover, they allow the control of the orientation and localization of subcellular organelles, cell polarity and signal transduction. Physical properties of the cell micro-environment, such as matrix rigidity, topography and geometry, modulate biochemical cues mediated by these molecular networks [19].

The self-assembly of molecular complexes, structured at the nano and microscale, is the underlying basis of the formation of cell adhesions, whether to synthetic biomaterials or to the natural ECM. Molecular processes that physically connect the ECM to the cell cytoskeleton regulate the adhesion to the matrix. Moreover, cell adhesion to the ECM has a significant role in regulating important cell phenotypes such as proliferation, apoptosis, differentiation, endocytosis, motility, matrix degradation and remodelling. The processes controlling cellular sensing of the physical microenvironment depend on sensing of its nanoscale physical properties, such as nanoscale geometry, nanotopography and nanoscale mechanics [19].

3. Materials and Methods

3.1. Poly(ethylene glycol) PEG

In this work, PEG Diacylate (PEGDA) and 8-arm PEG were used. The PEGDA, referred to as PEG_{575} was purchased from Sigma-Aldrich, with a molecular weight (Mw) of 575 Da, provided as a liquid pre-polymer. The 8-arm PEG-OH with a Mw of 15 KDa, referred to as 8PEG, was purchased from Jenkem technology USA and put through an acrylation process prior to its use in order to add acrylate groups to the terminal ends of the polymer chains and obtain UV-curable polymer. Both polymers were subjected to UV polymerization.

8PEG Acrylation

All reagents used were purchased from Sigma-Aldrich, unless stated otherwise. The acrylation procedure was done following the method described by Z. Zhang at the Lensen Lab group [20]. It starts with the 8PEG and the catalyst K_2CO_3 being dried separately in a vacuum oven at 95°C for 4 hours. A reflux column was set up on the reaction flask. In order to avoid the presence of humidity throughout the reaction, air was removed by bubbling through a nitrogen (N_2) flow, followed by the addition of the catalyst, dichloromethane anhydrous (DCM), and acryloyl chloride to the reaction flask. The reaction was carried out at 51°C and in absence of light for at least 3 days to ensure maximal conversion. The resulting products went through a filtration process in order to eliminate the remaining catalyst. The solvent was evaporated using a N_2 stream.

The filtered polymer was dropped into a beaker containing cold petroleum ether, resulting in its precipitation. The remaining acryloyl chloride was dissolved in petroleum ether. The precipitate was resuspended in DCM and poured into a sedimentation funnel with a small amount of a saturated solution of NaCl in distilled water. The organic phase dried over $MgSO_4$. After overnight drying, the $MgSO_4$ was filtered and a small amount of 4-methoxyphenol was dissolved into the filtrate, which acted as an inhibitor and avoided undesired polymerization during storage. Finally, the flask was placed on a rotary evaporator Hei-VAP Value (Heidolph Instruments GmbH & Co. KG, Germany) and left until the solvent was removed. The acrylated 8PEG was stored in a flask, under 6°C and kept away from the light.

3.2. AuNPs Synthesis and Seeded Growth

All chemicals used were purchased from Sigma Aldrich and used as received unless stated otherwise. The synthesis of the citrate capped AuNP seeds was done following the method described by Bastus et al.[21]. Intitially, a 2.2 mM solution of trisodium citrate in deionized water (150 ml) was heated in a three-necked round bottom flask fro 15 minutes. The solution was kept under vigorous stirring until achieving its boiling point. A condenser was used to prevent evaporation of the solvent. Afterwards, 1 mL of a solution containing 25 mM of $H[AuCl_4] \cdot 3H2O$ (precursor solution) was added to the solution of trisodium citrate. This resulted in a pink mixture that was kept stirring under reflux for an additional 10 minutes.

Right after the conclusion of the synthesis of AuNP seeds, the resulting product was cooled down until it reached a temperature of 90 °C. Afterwards, 1 mL of the 25 mM $H[AuCl_4] \cdot 3H2O$ solution was injected into the reaction. The mixture was kept under stirring for 30 min. This process was repeated two times. After the third addition of the precursor, the AuNPs solution was diluted by extracting 55 mL of the AuNPs solution and adding 53 mL of deionized water and 2 mL of a solution of 60 mM trisodium citrate. This solution was then used as the seed for the subsequent growing step, having the whole process been repeated again. The reaction temperature was maintained at 90 °C during the growing steps. In that way, depending on the number of growing steps, spherical Au NPs with diameters from 20 up to 200 nm were possible to achieve. For this work, particles with a diameter of 30-40 nm were used, referred to as batch 6.G4.

3.3. Gold Magnetic Nanoparticles

The gold magnetic nanoparticles (AuMNPs) used in this work were NITmagold Cit 50nm particles purchased from nitparticles, Zaragoza, Spain. The surface of the particles is coated with citrate anions, and the average particle diameter is 51.8 ± 6.1 nm. The solution had a molar concentration of 0.05 nM, with a particle concentration of 3.2×10^10 particles/mL and a peak SPR wavelength at 536 nm.

3.4. Blank Hydrogel Films Preparation

A photo-initiatior (PI) 2-hydroxy-4'-(2-hydroxyethoxy)-2-methylpropiophenone, M_W 224.26 $gmol^{-1}$, purchased from Sigma-Aldrich, was added to all PEG-based polymers. The concentration of PI is expressed in weight percentage with respect to the quantity of polymer.

1%wt of PI was added to a flask, together with 0.2 g of the polymer (PEG_{575}, 8PEG or PEG_{575}-8PEG Blend in a 1:1 ratio). For the PEG_{575} and 8PEG, the flask was put under sonication for 10 minutes, to promote the dissolution of the PI in the hydrogel. For the polymers in solid state, the flask was first put on a heating plate at 80°C until the hydrogel melted. For the Blend material, it was kept under stirring while being heated. Few drops of the mixtures were then put on a microscope glass using a glass pipette, and covered with a thin glass. For the polymers in solid state at room temperature, the microscope glass and the pipette

were pre-heated at 80°C before handling. The mixtures was put to cure under UV light 366 nm, under a N_2 atmosphere in absence of O_2 for 18 minutes.

3.5. Nanocomposite Hydrogel Films Preparation

A photo-initiatior (PI) 2-hydroxy-4'-(2-hydroxyethoxy)-2-methylpropiophenone, M_W 224.26 $gmol^{-1}$, purchased from Sigma-Aldrich, was added to all PEG-based polymers. The concentrations of PI, AuNPs and AuMNPs are expressed in weight percentage with respect to the quantity of polymer. The procedures for the nancomposites containing AuNPs and AuMNPs differ only on the application of a magnet during UV-curing.

1%wt of PI was added to a flask, together with 40%wt of AuNPs or AuNMPs solution and with 0.2 g of the polymer (PEG_{575}, 8PEG or PEG_{575}-8PEG Blend in a 1:1 ratio). For the PEG_{575} and 8PEG, the flask was put under sonication for 30 minutes, to promote the dissolution of the PI and the dispersion of the AuNPs or AuMNPs in the hydrogel. For the polymers in solid state, the flask was first put on a heating plate at 80°C until the hydrogel melted. For the Blend material, it was kept under stirring while being heated. Few drops were then put on a microscope glass and covered with a thin glass. For the polymers in solid state at room temperature, the microscope glass and the pipette were pre-heated at 80°C before handling. For case of PEG_{575} AuMNP NC film, it was placed on top of a magnet for 15 minutes prior to UV-curing. The NC films were cured under UV light (366 nm) in a N_2 atmosphere in absence of O_2 for 20 minutes (for AuNP NCs) and 25 minutes (for AuMNP NCs). The AuMNPs mixtures were UV cured in the presence of a magnet under the microscope glass.

3.6. Cell Culture

Mouse fibroblasts L929 (provided by Dr. Lehmann, Fraunhofer Institute for Cell Therapy and Immunology, IZI, Leipzig, Germany) were cultured in RPMI 1640 medium with addition of 10% Fetal Bovine Serum (FBS) and 1% Penicillin/Streptomycin (PS) in an incubator CB150 Series (Binder GmbH, Germany) at controlled temperature (37°C) and CO_2 atmosphere (5%). Medium, sera and reagents were provided by PAA Laboratories GmbH, Germany, unless stated otherwise.

3.7. Analytical Methods

Swelling Experiments

The following procedure was adapted from Zustiak et al. [22]. For each sample, the degree of swelling was measured to estimate certain structural parameters, namely: molecular weight between cross-links, effective cross-link density, and mesh size. Hydrogel swelling is a function of network structure, degree of cross-linking, as well as hydrophilicity. Firstly, the dry mass (M_D) of the hydrogels was measured. The hydrogel films were then incubated at 37°C in deionized water for 24 hours, and the weight after swelling (M_S) was measured. The swelling ratio based on the hydrogel mass (Q_M) was calculating using the following equation:

$$Q_M = \frac{M_S}{M_D}. \tag{2}$$

Q_M was then further used to calculate the volume swelling ration Q_V:

$$Q_V = 1 + \frac{\rho_p}{\rho_s}(Q_M - 1), \tag{3}$$

where ρ_p is the density of the hydrogel (1.12 g/cm^3 atfor PEG [23]) and ρ_s is the density of the solvent (1 g/cm^3 for water). To determine the hydrogel mesh size (ξ), Flory-Rehner calculations were used [24]. First, the molecular weight between cross-links (M_c) was calculated by:

$$\frac{1}{\overline{M}_c} = \frac{2}{\overline{M}_n} - \frac{\frac{\overline{v}}{V_1}(ln(1-v_2) + v_2 + \chi_1 v_2^2)}{v_2^{1/3} - \frac{v_2}{2}}, \tag{4}$$

where $\overline{M}_n$ is the number-average molecular weight of the un-cross-linked hydrogel (the molecular weight of the polymer), V_1 is the molar volume of the solvent (18 cm^3/mol for water), v_2 is the polymer volume fraction in the equilibrium swollen hydrogel, which is equal to the reciprocal of Q_V, $\overline{v}$ is the specific volume of the polymer (ρ_p/ρ_s), and χ_1 is the polymer-solvent interaction parameter (0.426 for PEG-water) and assumed constant. The mesh size of the network was then determined following the procedure described by Canal and Peppas [25], where the root-mean-square end-to-end distance of the polymer chain in the unperturbed state ($(\overline{r}_0^2)^{1/2}$) was calculated as follows:

$$(\overline{r}_0^2)^{1/2} = lC_n^{1/2}n^{1/2}, \tag{5}$$

where l is the average bond length (0.146 nm), C_n is the characteristic ratio of the polymer (typically 4.0 for PEG) and n is the number of bonds in the cross-link:

$$n = 2\frac{\overline{M}_c}{M_r}, \tag{6}$$

where M_r is the molecular weight of the repeat unit (44 for PEG), and the mesh size could then be calculated by:

$$\xi = v_2^{-1/3}(\overline{r}_0^2)^{1/2}. \tag{7}$$

Atomic Force Microscopy

Topographical imaging was performed in intermittent contact mode and force mapping was done in contact mode for dry measurements and intermittent mode for underwater measurements. AFM analysis was done using Nanowizard II, JPK instruments.

Transmission Electron Microscopy

TEM images were acquired using a TECNAI $G^2$20 S-TWIN microscope operating at 200 kV with a point of resolution of 0.24 nm.

Scanning Electron Microscopy

SEM imaging was performed on a LEO 982 offered by ZEISS Company, the optical parts of the microscope being from GEMINI Optics. The samples were carbon-coated and the measurements were performed using an Inlens detector operating at 20.0 kV and 10 kV.

4. Results

4.1. Gold Nanoparticles Synthesis

From the TEM imaging of a sample from 6.G4 batch (Figure 1 (a)), it is possible to see that the synthesized AuNPs are spherical. Using ImageJ program, the size distribution of the nanoparticles was calculated, presenting diameters between 25 and 40 nm, with a mean value of 30 nm and a standard deviation of 3.13. The UV-Vis spectrum shows an SPR peak at 527 nm corresponding to a maximum absorbance of 0.97 (Figure 1 (b)). Using the Lambert-Beer equation defined as $A = \epsilon lc$, where A is the maximum absorbance, ϵ the extinction coefficient for AuNPs (6.06×10^9 [26]), and l the length of the cuvette (1 cm), it was possible to calculate a molar concentration (c) of 0.16 nM.

4.2. Surface Topography

The images were processed using JPK Data Processing program and can be found in the Appendix in the end of the document. The RMS (root mean square) roughness presented is an average value of 10 measurements made in arbitrary directions with a length of 10 μm.

Blank Hydrogel Films

Initially, blank samples of the hydrogels were synthesized and analyzed in order to understand the topography of the surface when there were no nanoparticles present in their volume and allow the comparison between the hydrogel itself and the NC hydrogel. Figure 2 A-C shows the height images of the lower surface of the blank hydrogel films. The three blank samples show a relatively smooth surface with an RMS roughness (Rq) of 840.4 pm for PEG_{575}, 554.5 pm for 8PEG and 860.2 pm for the Blend material. The small height deviations resembling particles in the PEG_{575} and 8PEG samples may be due to impurities present in the instruments used to prepare the samples or present in the surrounding environment, that got transferred to the samples.

AuNP NC Hydrogel Films

Given the possibility of detecting AuNPs in the surface of the hydrogel film, these were expected to be more visible on the lower surface of the films, due to gravitational forces that could stimulate particles to deposit. Figure 3 A-C show the height profile of the lower surfaces of the AuNP NC hydrogels. For PEG_{575} (Figure 3 - A), the height profile of the lower surface is not consistent with the presence of any particles, and showed an RMS roughness of 1.6 nm, which is slightly higher when compared to the blank PEG_{575} film and may indicate the presence of AuNPs in the volume of the hydrogel. The height image for the 8PEG AuNP NC film (Figure 3 - B) shows the presence of elongated particles. It is not expected for these to be AuNPs, as they are supposed to show a shperical profile. These elongated particles are very similar to the ones found on the surface of the blank 8PEG sample, which may indicate that these are topographies created by the crystalization of 8PEG. The RMS roughness of the lower surface of the hydrogel film is 1.0 nm, being only slightly higher when comparing to the blank 8PEG film. This can be explained by the same reasons pointed out for the case of PEG_{575} films.

For the 8PEG-PEG_{575} Blend material, it is possible to observe small particles present in the lower surface of the hydrogel film (Figure 3 - C). These show a spherical profile, consistent with the shape of the AuNPs, and the surface presents a slightly bigger height difference measured (7.06 nm). These may be AuNPs embedded or entrapped within the hydrogel matrix, and are unlikely to have their surface exposed. The RMS roughness of the lower surface of the 8PEG AuNP NC film is 646.6 pm, which is lower than the RMS roughness measured in the blank 8PEG film. This may be due to the effect that adding AuNPs in solution to the pre-curing mixture has in the retardation on the re-solidification of 8PEG after melting and handling, as it helps on the dissolution of the solid hydrogel.

AuMNP NC Hydrogel Films

Since the density of particles being detected in the surface of the films using AuNPs was very low, a

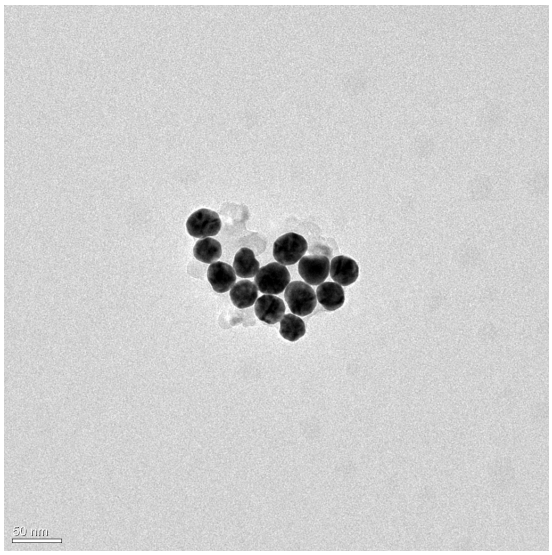

(a) TEM Image of the 6.G4 batch of AuNPs

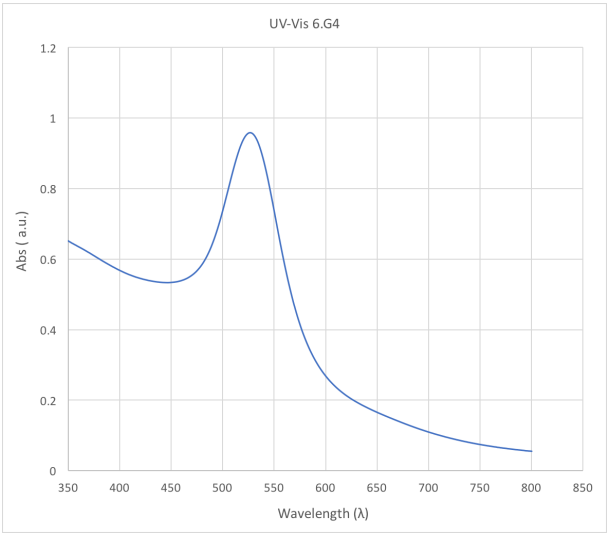

(b) UV-Vis spectrum of 6.G4 batch of AuNPs

Figure 1: TEM image (a) and UV-Vis spectrum of 6.G4 batch of the synthesized AuNPs (b).

new strategy was thought of by introducing the use of AuMNPs. These particles would still have the gold necessary to promote cell adhesion to the films, and possessed magnetic properties that allowed the use of a magnet to force the particles to migrate to a specific area of the hydrogel.

In order to attempt to pull the AuMNPs to the lower surface of the hydrogel films, a magnet was placed under the pre-cured gels. In the case of the PEG_{575} AuMNP NC, it was possible to leave the sample in contact with the magnet some time before the curing, as it is in liquid state at room temperature, with the goal of enhancing the migration of the nanoparticles to the bottom of the gel. In Figure 4 - A, it is possible to see several spherical particles that resemble the AuMNP that were expected to be detected. However, the heights detected, considering the diameter of 50 nm of the nanoparticles, is quite lower than expected, being the highest peak detected in the cross-section around 12 nm. This can indicate that the particles are embedded in the gel. The RMS roughness of this surface is 2.0 nm.

On the lower surface of the 8PEG AuMNP NC film (Figure 4 - B), a bigger density of particles can be detected, with heights around 10 nm. The profile of the particles detected is similar to the one observed in the PEG_{575} AuMNP NC sample, which can indicate that these are indeed nanoparticles. Their elongated shape may be due to imaging artifacts. The lower surface of the 8PEG AuMNP NC film has a RMS roughness of 2.8 nm.

Regarding the Blend sample, contrary to what was expected, it is not possible to detect a significant density of particles present in the surface of the film (Figure 4 - C). The fact that no particles were detected may be associated by the fact that this is a local characterization method, and it may have happened that the measurements were not made on areas where AuNPs were indeed present. Also, because the magnet has to be placed at the same time as the film is being cured, as it is not liquid at room temperature, the fast polymerization of the film may not allow the particles to completely migrate to the bottom. This surface has an RMS roughness of 1.7 nm, which is higher than the blank Blend material. This may indicate the presence of particles embedded under the material that were not able to fully migrate to the bottom of the film.

4.3. Swelling Behaviour

In order to calculate the swelling parameters of the hydrogel films, 3 individual samples of each film were weighed in dry state, incubated at 37°C in deionized water, and weighed again after 24 hours of incubation, in swollen state. Table 1 shows the parameters calculated through the methods described previously.

Looking first at the swelling ratios, both mass (Q_M) and volume (Q_V) based, it is possible to see that the PEG_{575} and Blend materials are the ones that have higher ratios. This means that these materials swell less than the 8PEG materials, as it can be also observed by the %S values. Comparing the blank samples with the NC samples, the materials in which it is seen a bigger difference in its swelling behaviour are the 8PEG, that has an increase in its swelling ratios when nanoparticles are present in its volume, whilst the opposite happens with the PEG_{575} and Blend materials. This may be due to the difference in the structure of the polymer, as the presence of nanoparticles may affect differently

Table 1: Swelling ratio (Q_M), volume swelling ratio (Q_V) and mesh size (ξ) from blank, AuNP NC and AuMNP NC hydrogel samples

	Blank			**AuNP**			**AuMNP**		
	PEG	8PEG	Blend	PEG	8PEG	Blend	PEG	8PEG	Blend
$\%S$	40	313	57	48	135	69	63	237	112
Q_M	72 ± 7	21±3	64±6	68±9	43±4	60±8	64±15	30±5	47±5
Q_V	69±8	15±4	60±7	65±10	36±5	55±9	60±17	22±5	41±5
ξ ($\AA$)	3.9±0.9	72.7±25.6	5.6±1.4	4.4±1.5	14.6±3.2	6.7±2.1	5.5±2.9	33.2±12.9	11.5±2.3

the crosslinkage of the polymers.

In the case of 8PEG, the presence of nanoparticles in its structure induces a decrease of water intake. As for the PEG_{575} and Blend materials, the presence of nanoparticles may decrease the level of crosslinkage, allowing the polymer to have a bigger water intake, as a higher degree of crosslinking of a polymer may increase its resistance to solvents [27].

The AuNP NC materials show a slightly higher swelling ratio than their AuMNP equivalents. This may be due to the fact that most of the AuMNP are concentrated in a portion of the hydrogel film, as they were forced to migrate to the bottom of the film, and the migration might affect the crosslinking process by decreasing its rate, which allows the hydrogel to swell more.

It is also important to refer that the possible presence of impurities in the samples may affect the swelling behaviour of the hydrogels, as well as the human error associated to the measurements made.

4.4. Force Mapping

The measurements were made on the lower side of the films. Force mapping was performed in contact mode using CONTGD-G tips with a half-cone angle of 10° at the apex, on a 10×10μm area with 8×8 pixels, which allows to determine 64 values of E for each sample, being the values presented a mean value of those. The calibration was done using glass and 3 different values for InvOLS and spring constant k were measured. For the underwater measurements, the samples were submerged in deionized water, left to swell for 20 minutes and then measured.

In both dry and swollen measurements (Tables 2 and 3), the materials based only on PEG_{575} showed to be the stiffest and 8PEG the softest. When analyzing their behavior upon the presence of nanoparticles, the NC films all showed a slightly decrease in E, on both AuNP and AuMNP cases. This can be explained due to the fact that in both cases, the nanoparticles were not functionalized with groups that allowed to cross-link with the acrylate groups of the gels. This may have inhibited the crosslinking of the gel, resulting in materials with lower stiffness.

AuMNP NCs show slightly higher values for E in the swollen state than in the dry state. This can be due to the fact that, when the gel swells, the particles get closer to the surface, resulting in a stiffer profile. The PEG_{575} and Blend AuNP NCs measured in the wet state have higher values than the ones measured in the dry state, which can be explained by the same reason presented for the AuMNP NCs. However, the values in both measurements do not differ too much, and this may be due to the fact the the gels are not left underwater enough time to swell to a significant extent.

The relatively high values observed for the standard deviations (SD), especially in the cases of the AuMNP NCs, are explained by the wide range of values measured for E in each of the 64 points of measurement done in the sample. This range may happen due the difference in stiffness between measuring a surface containing only gel and a surface containing a nanoparticle, resulting in a set of values that may differ in orders of magnitude.

4.5. Cell Adhesion

Cell culture was performed on the samples using L929 fibroblasts. After 24 hours of incubation with a concentration of 40 000 cells/mL at 37C and in at atmosphere of 5% CO_2, the samples were analyzed under a ZEISS microscop, the images processed using the AxioVision (ZEISS) program and can be found in the Appendix in the end of the document. Figure 5 shows the control cells from 3 different wells in the tissue culture polystyrene (TCPS). It is possible to observe that after 24 hours of incubation, most of the cells are widely spread and adhered to the TCPS.

Figures 6-8 show images of the cells cultured in the blank hydrogels, AuNP NC hydrogels and AuNMP NC hydrogels. A spherical morphology indicates that the cells did not adhere to the substrate, whilst spreading indicates adhesion. Most

Table 2: Young's Modulus (E) and respective standard deviation (SD) from hydrogel samples in dry state

	Blank			**AuNP**			**AuMNP**		
	PEG	8PEG	Blend	PEG	8PEG	Blend	PEG	8PEG	Blend
$E(Pa)$	4.65E+08	3.45E+07	1.41E+08	1.69E+08	2.78E+07	9.38E+07	2.14E+08	2.43E+07	5.03E+07
SD	2.42E+07	4.14E+06	1.05E+07	3.37E+07	3.32E+06	9.06E+06	1.28E+07	1.29E+07	6.08E+06

Table 3: Young's Modulus (E) and respective standard deviation (SD) from hydrogel samples in swollen state

	Blank			**AuNP**			**AuMNP**		
	PEG	8PEG	Blend	PEG	8PEG	Blend	PEG	8PEG	Blend
$E(Pa)$	4.00E+08	2.12E+07	1.91E+08	2.57E+08	2.07E+07	1.36E+08	2.61E+08	3.07E+08	6.46E+07
SD	1.24E+07	1.16E+06	7.46E+07	5.89E+07	1.09E+06	1.03E+08	2.94E+07	5.53E+08	1.74E+07

of the samples did not promote spreading of the cells, with the exception of the AuMNP PEG_{575} NC, where the biggest amount of particles was detected on the topographical analysis. Some samples show some initial signs of adhesion, as is the case of the AuNP samples. In general, the low adhesion can be explained with the lack of gold being exposed to the surface, thus not allowing cells to be directly in contact with it and triggering cell adhesion mechanisms. Some of the initial adhesion observed might be due to topographical inconsistencies or rigidity patterns formed due to non-homogeneous mixes of the gels (in the case of the Blend materials), or non homogeneous distribution of particles. Cells respond to physical patterns and tend to migrate and adhere to surfaces with an increased rigidity, a phenomenon known as durotaxis [28].

5. Conclusions

This work has contributed for the further understanding of how mechanical and physical properties of PEG-based hydrogels can be manipulated and tailored in order to confer them certain characteristics that influence cell adhesion.

The incorporation of AuNPs into different types of PEG-based hydrogels has shown to affect the mechanical properties and swelling behaviour of the materials, as well as their topographical and structural profile. However, it was not possible to detect a relevant number of particles present at the surface of the hydrogel films, whilst for the AuMNPs these were possible to detect in the PEG_{575} and 8PEG based gels. The presence of nanoparticles in general did not enhance the stiffness of the materials but enhanced their swelling capacity, possibly due to the fact that the presence of the particles may interfere with the crosslinking efficiency of the hydrogels. Regarding cell adhesion, materials where more gold particles were detected at the surface showed to promote cell adhesion more than in materials where particles were embedded in the film.

Future studies on the effects that the nanoparticles have on the crosslinking density, as well as their level of dispersion on the gel should be conducted. Moreover, the effect that the thermal and electrical properties of the nanoparticles might have on the materials can be further explored. The application of patterning techniques to these materials, such as MIMIC (micro-molding in capillaries) or FIMIC (fill-molding in capillaries), could also allow further understanding of their impact on cell adhesion.

Overall, it was possible to adopt simple and quick approaches to prepare NC hydrogel films by combining PEG with AuNPs and AuMNPs. Their characterization has helped to enhance the further understanding of the nature of the properties acquired by the hydrogels by incorporating AuNPs and AuMNPs, and their impact on triggering cell adhesion mechanisms.

References

[1] D. F. Williams. B. In *TheWilliamsDictionary of Biomaterials*, pages 33–54. Liverpool University Press, 1999.

[2] Allan S. Hoffman. Hydrogels for biomedical applications. *Advanced Drug Delivery Reviews*, 64:18–23, dec 2012.

[3] O. WICHTERLE and D. LÍM. Hydrophilic gels for biological use. *Nature*, 185(4706):117–118, jan 1960.

[4] Sytze J. Buwalda, Kristel W.M. Boere, Pieter J. Dijkstra, Jan Feijen, Tina Vermonden, and Wim E. Hennink. Hydrogels in a historical perspective: From simple networks to smart materials. *Journal of Controlled Release*, 190:254–273, sep 2014.

[5] Gonzalo de Vicente and Marga C. Lensen. Topographically and elastically micropatterned PEG-based hydrogels to control cell adhesion and migra-

tion. *European Polymer Journal*, 78:290–301, may 2016.

[6] Marga C. Lensen, Vera A. Schulte, Jochen Salber, Mar Diez, Fabian Menges, and Martin Möller. Cellular responses to novel, micropatterned biomaterials. *Pure and Applied Chemistry*, 80(11), jan 2008.

[7] Fang Ren, Cigdem Yesildag, Zhenfang Zhang, and Marga C. Lensen. Functional PEG-hydrogels convey gold nanoparticles from silicon and aid cell adhesion onto the nanocomposites. *Chemistry of Materials*, 29(5):2008–2015, feb 2017.

[8] N Peppas. Hydrogels in pharmaceutical formulations. *European Journal of Pharmaceutics and Biopharmaceutics*, 50(1):27–46, jul 2000.

[9] Enas M. Ahmed. Hydrogel: Preparation, characterization, and applications: A review. *Journal of Advanced Research*, 6(2):105–121, mar 2015.

[10] Kristi S. Anseth, Christopher N. Bowman, and Lisa Brannon-Peppas. Mechanical properties of hydrogels and their experimental determination. *Biomaterials*, 17(17):1647–1657, jan 1996.

[11] Xiaju Cheng, Xin Tian, Anqing Wu, Jianxiang Li, Jian Tian, Yu Chong, Zhifang Chai, Yuliang Zhao, Chunying Chen, and Cuicui Ge. Protein corona influences cellular uptake of gold nanoparticles by phagocytic and nonphagocytic cells in a size-dependent manner. *ACS Applied Materials & Interfaces*, 7(37):20568–20575, sep 2015.

[12] Junmin Zhu and Roger E Marchant. Design properties of hydrogel tissue-engineering scaffolds. *Expert Review of Medical Devices*, 8(5):607–626, sep 2011.

[13] W.E Hennink and C.F van Nostrum. Novel crosslinking methods to design hydrogels. *Advanced Drug Delivery Reviews*, 54(1):13–36, jan 2002.

[14] Praveen Thoniyot, Mein Jin Tan, Anis Abdul Karim, David James Young, and Xian Jun Loh. Nanoparticle-hydrogel composites: Concept, design, and applications of these promising, multifunctional materials. *Advanced Science*, 2(1-2):1400010, jan 2015.

[15] Yuxi Xu, Kaixuan Sheng, Chun Li, and Gaoquan Shi. Self-assembled graphene hydrogelviaa one-step hydrothermal process. *ACS Nano*, 4(7):4324–4330, jul 2010.

[16] Su Ryon Shin, Sung Mi Jung, Momen Zalabany, Keekyoung Kim, Pinar Zorlutuna, Sang bok Kim, Mehdi Nikkhah, Masoud Khabiry, Mohamed Azize, Jing Kong, Kai tak Wan, Tomas Palacios, Mehmet R. Dokmeci, Hojae Bae, Xiaowu (Shirley) Tang, and Ali Khademhosseini. Carbon-nanotube-embedded hydrogel sheets for engineering cardiac constructs and bioactuators. *ACS Nano*, 7(3):2369–2380, mar 2013.

[17] Christopher A. Holden, Puneet Tyagi, Ashish Thakur, Rajendra Kadam, Gajanan Jadhav, Uday B. Kompella, and Hu Yang. Polyamidoamine dendrimer hydrogel for enhanced delivery of antiglaucoma drugs. *Nanomedicine: Nanotechnology, Biology and Medicine*, 8(5):776–783, jul 2012.

[18] Azadehsadat Doulabi, Kibret Mequanint, and Hadi Mohammadi. Blends and nanocomposite biomaterials for articular cartilage tissue engineering. *Materials*, 7(7):5327–5355, jul 2014.

[19] Barry M Gumbiner. Cell adhesion: The molecular basis of tissue architecture and morphogenesis. *Cell*, 84(3):345–357, feb 1996.

[20] Zhenfang Zhang. *Synthesis and characterization of 8 arm-Poly(ethylene glycol) Based hydrogels via Michael addition or click chemistry for Biomedical Applications*. PhD thesis, Technische Universitat Berlin, 2015.

[21] Neus G. Bastus, Marcelo J. Kogan, Roger Amigo, Dolors Grillo-Bosch, Eyleen Araya, Antonio Turiel, Amilcar Labarta, Ernest Giralt, and Victor F. Puntes. Gold nanoparticles for selective and remote heating of -amyloid protein aggregates. *Materials Science and Engineering: C*, 27(5-8):1236–1240, sep 2007.

[22] Silviya P. Zustiak and Jennie B. Leach. Hydrolytically degradable poly(ethylene glycol) hydrogel scaffolds with tunable degradation and mechanical properties. *Biomacromolecules*, 11(5):1348–1357, 2010.

[23] Donald L Elbert, Alison B Pratt, Matthias P Lutolf, Sven Halstenberg, and Jeffrey A Hubbell. Protein delivery from materials formed by self-selective conjugate addition reactions. *Journal of Controlled Release*, 76(1-2):11–25, sep 2001.

[24] Sanxiu Lu and Kristi S. Anseth. Release behavior of high molecular weight solutes from poly(ethylene glycol)-based degradable networks. *Macromolecules*, 33(7):2509–2515, apr 2000.

[25] Tiziana Canal and Nikolaos A. Peppas. Correlation between mesh size and equilibrium degree of swelling of polymeric networks. *Journal of Biomedical Materials Research*, 23(10):1183–1193, oct 1989.

[26] Xiong Liu, Mark Atwater, Jinhai Wang, and Qun Huo. Extinction coefficient of gold nanoparticles with different sizes and different capping ligands. *Colloids and Surfaces B: Biointerfaces*, 58(1):3–7, jul 2007.

[27] Lawrence E. Nielsen. Cross-linking–effect on physical properties of polymers. *Journal of Macromolecular Science, Part C: Polymer Reviews*, 3(1):69–103, jan 1969.

[28] Chun-Min Lo, Hong-Bei Wang, Micah Dembo, and Yu li Wang. Cell movement is guided by the rigidity of the substrate. *Biophysical Journal*, 79(1):144–152, jul 2000.

Appendix - Topography and Cell Culture Images

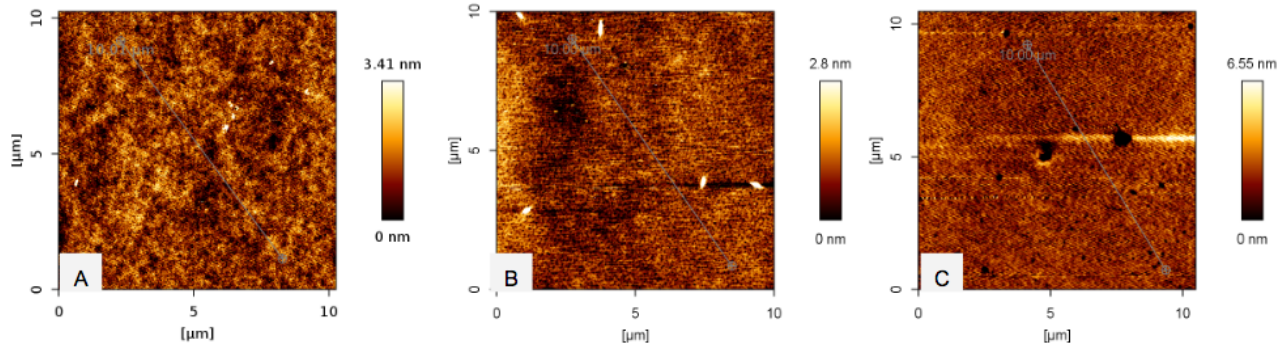

Figure 2: Height image of the lower surface of blank hydrogel films: A - PEG_{575}, B - 8PEG, C - Blend

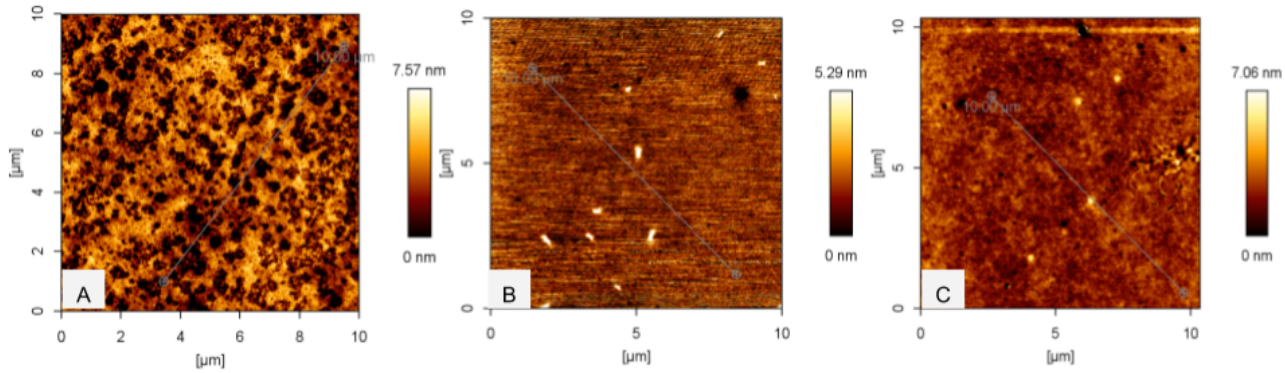

Figure 3: Height image of the lower surface of AuNP NC hydrogel films: A - PEG_{575}, B - 8PEG, C - Blend

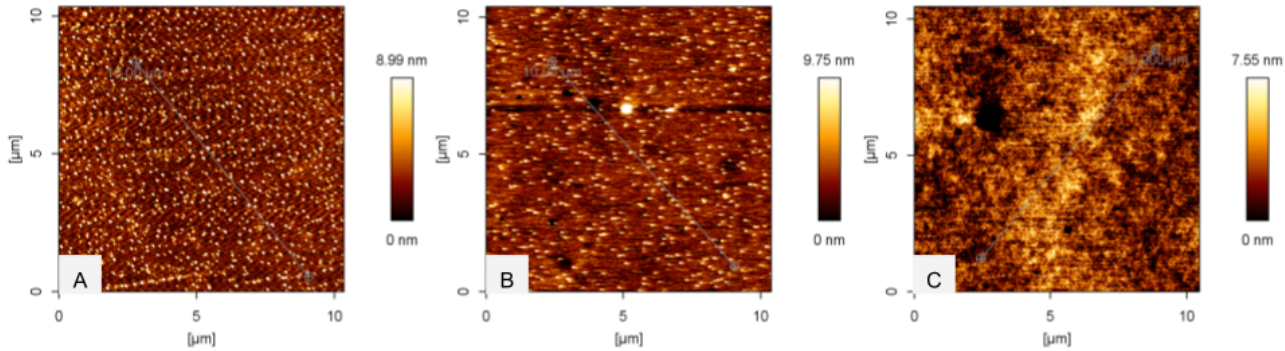

Figure 4: Height image of the lower surface of AuMNP NC hydrogel films: A - PEG_{575}, B - 8PEG, C - Blend

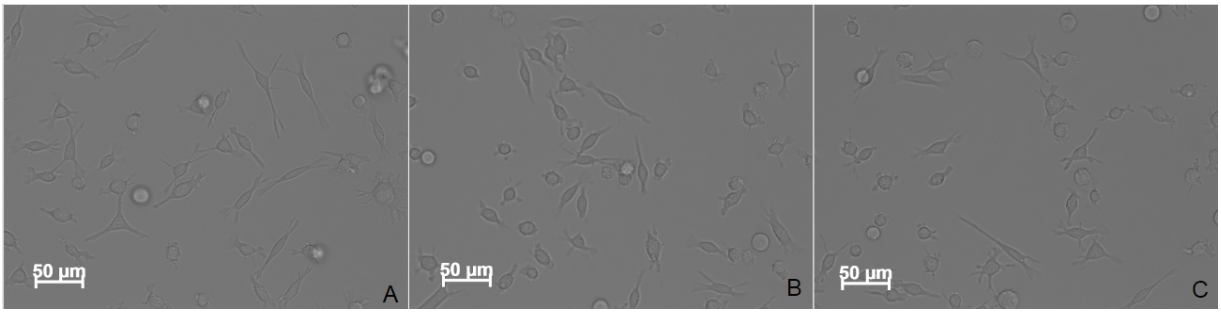

Figure 5: Control cells cultured in 3 different culture plates (A, B and C)

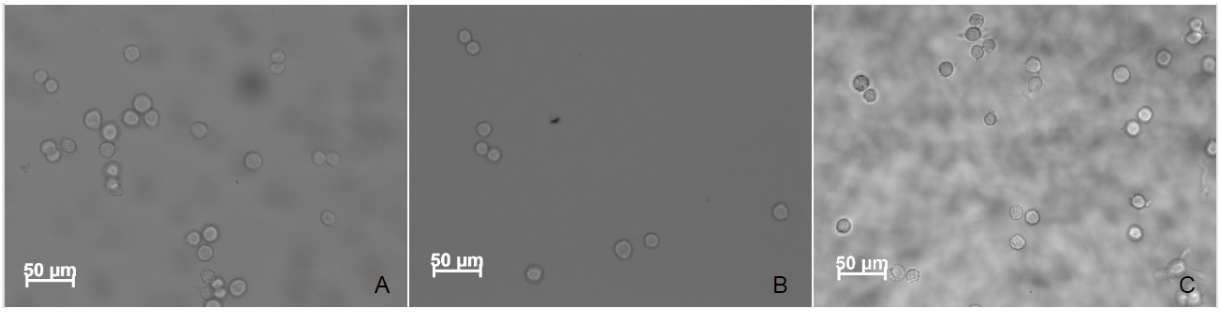

Figure 6: L929 cells cultured in PEG_{575} (A), 8PEG (B) and Blend (C) blank hydrogel samples

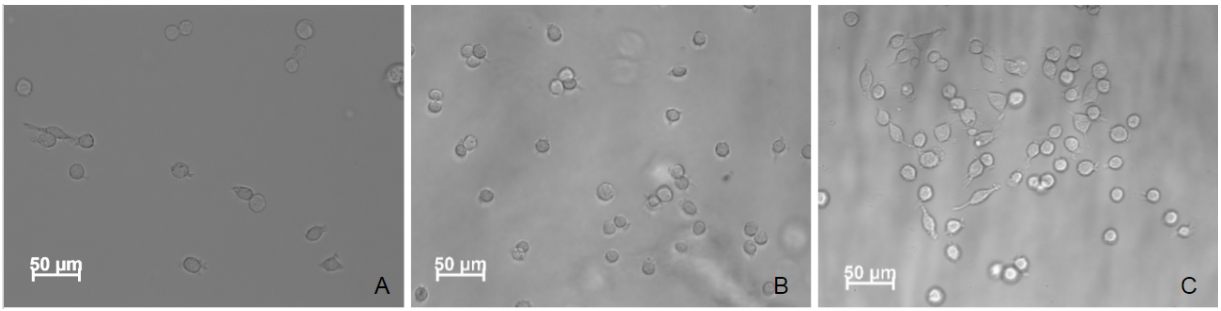

Figure 7: L929 cells cultured in PEG_{575} (A), 8PEG (B) and Blend (C) AuNP NC hydrogel samples

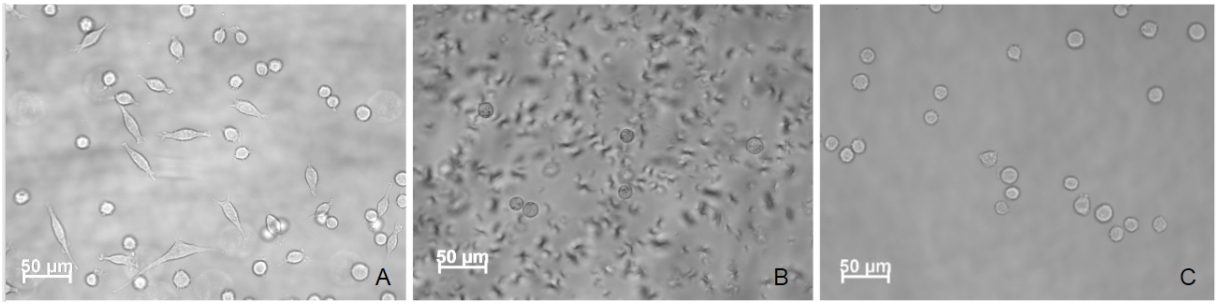

Figure 8: L929 cells cultured in PEG_{575} (A), 8PEG (B) and Blend (C) AuMNP NC hydrogel samples